LANGMUIR

pubs.acs.org/Langmuir Article

Plasma Activation of Microplates Optimized for One-Step Reagent-Free Immobilization of DNA and Protein

Kanako Coffi Dit Gleize, Clara T. H. Tran,* Anna Waterhouse,* Marcela M. M. Bilek, and Shelley F. J. Wickham*

Cite This: *Langmuir* 2023, 39, 343−356 Read Online

ACCESS | Metrics & More | Article Recommendations | Supporting Information

ABSTRACT: Activated microplates are widely used in biological assays and cell culture to immobilize biomolecules, either through passive physical adsorption or covalent cross-linking. Covalent attachment gives greater stability in complex biological mixtures. However, current multistep chemical activation methods add complexity and cost, require specific functional groups, and can introduce cytotoxic chemicals that affect downstream cellular applications. Here, we show a method for one-step linker-free activation of microplates by energetic ions from plasma for covalent immobilization of DNA and protein. Two types of energetic ion plasma treatment were shown to be effective: plasma immersion ion implantation (PIII) and plasma-activated coating (PAC). This is the first time that PIII and PAC have been reported in microwell plates with nonflat geometry. We confirm that the plasma treatment generates radical-activated surfaces at the bottom of wells despite potential shadowing from the walls. Comprehensive surface characterization studies were used to compare the PIII and PAC microplate surface composition, wettability, radical density, optical properties, stability, and biomolecule immobilization density. PAC plates were found to have more nitrogen and lower radical density and were more hydrophobic and more stable over 3 months than PIII plates. Optimal conditions were obtained for high-density DNA (PAC, 0 or 21% nitrogen, pH 3−4) and streptavidin (PAC, 21% nitrogen, pH 5−7) binding while retaining optical properties required for typical high-throughput biochemical microplate assays, such as low autofluorescence and high transparency. DNA hybridization and protein activity of immobilized molecules were confirmed. We show that PAC activation allows for high-density covalent immobilization of functional DNA and protein in a single step on both 96- and 384-well plates without specific linker chemistry. These microplates could be used in the future to bind other user-selected ligands in a wide range of applications, for example, for solid phase polymerase chain reaction and stem cell culture and differentiation.

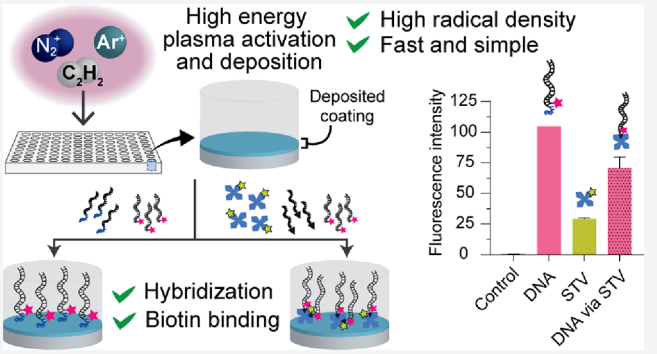

INTRODUCTION

Microplates are a critical and ubiquitous platform for high-throughput biological assays and cell culture.[1] Applications include enzyme-linked immunosorbent assays (ELISAs),[2,3] biomolecule interaction studies,[4] and cell−drug interaction screening.[5] The standardized microplate format facilitates rapid optical characterization and automation. Microplates are typically made of polystyrene, which has good optical properties but is hydrophobic and does not adhere to cells or biomolecules well. Modified plates, known as tissue culture-treated plates, are treated with oxygen plasma to reduce hydrophobicity and enhance cell adhesion.[6] However, this basic tissue culture oxygen treatment is not sufficient for a growing range of techniques where high-stability and high-density biomolecule surface immobilization is required. For example, collagen type I-coated plates can be used to isolate muscle-derived stem cells,[7] while culture on E-cadherin-coated plates can maintain embryonic stem cells in a pluripotent state.[8] A limited range of chemically functionalized microplates are commercially available but require multistep attachment methods, lack flexibility of functional groups, and are expensive. Commercial protein-coated microplates are similarly expensive and only available for a limited range of extracellular matrix proteins. Here, we develop new methods for plasma activation of polystyrene microplates using plasma immersion ion implantation (PIII) and plasma-activated coating (PAC). This is the first report of PIII or PAC on nonflat polystyrene geometries such as microplates. We show that PIII and PAC allow for simple high-density and high-

Received: September 19, 2022
Revised: December 12, 2022
Published: December 22, 2022

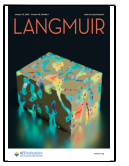

https://doi.org/10.1021/acs.langmuir.2c02573
Langmuir 2023, 39, 343−356

Table 1. Chemical Activation Methods for Covalent Immobilization of DNA and Corresponding DNA Hybridization Densities[a]

surface modification	attachment chemistry	substrate type	hybridization density (molecules/cm^2)
NHS-silane[10]	amine-DNA	silicon wafer	4.0×10^{10}
aminosilane[15]	cross-linked via SMPB	fused silica, silicon wafer	8.4×10^{10}
3-mercaptopropylsilane[16]	disulfide-DNA	glass slide	4.5×10^{12}
aminosilane[17]	cross-linked via SIAB	silicon wafer	6.0×10^{12}
polymerizable acrylic silane[18]	photochemical copolymerization with acrylamide	silica optical fiber	1.6×10^{13}

[a]The substrates used in these examples are not polystyrene and have not been applied on microplates.

stability immobilization of multiple types of biomolecules on microplates for a wide range of bioassays and cell culture applications at low cost.

Surface immobilization of biomolecules on a solid support can be achieved via physical adsorption or covalent binding. Physical adsorption is commonly used to attach biomolecules such as DNA and proteins to microplate surfaces through hydrophobic or electrostatic interactions. Although the technique is simple, physically adsorbed biomolecules bind weakly with a random orientation[9] and are sensitive to changes in ionic concentration, pH, heat, and detergent, reducing reproducibility.[10] Proteins can also be denatured by physical adsorption, for example, reducing monoclonal antibody activity to less than 10%.[11] For DNA, physical adsorption methods are unsuitable for applications in biosensing as they do not control the molecule orientation on the surface.[12]

Stronger, more specific binding can be achieved through covalent immobilization via chemical activation of microplates,[9] increasing stability, activity, and resistance to washing and reducing competitive protein exchange from the Vroman effect.[13] Silane chemistry, for example, aminopropyltriethoxylsilane (APTES), is often used for activation of surfaces for biomolecule binding.[14] This surface activation approach has been used in DNA microarrays where the DNA is functionalized with thiol or amine groups prior to chemical coupling to the surface.[10,15−17] The hybridized DNA density of such surfaces can range from 4.0×10^{10} to 6.0×10^{12} molecules/cm^2 (Table 1), while a denser hybridized DNA surface has been made by co-polymerization using acrylamide (1.6×10^{13} molecules/cm^2).[18] Microplate surfaces have also been previously functionalized with chitosan,[19] thiol groups,[20] or primary amine groups[21,22] for protein, enzyme, peptide, and *Escherichia coli* immobilization. However, chemical activation methods are multistep processes, often requiring modified biomolecules such as amine-modified or thiol-modified DNA oligonucleotides, and may involve cytotoxic reagents that generate chemical waste and must be completely removed from the surface before downstream applications in cell culture.[23]

Covalent immobilization of biomolecules in one step without chemical linkers is possible through radical-rich surfaces obtained from energetic ion plasma activation.[24] The physical treatment using the bombardment of energetic ions is fast and reproducible, and the reactivity of these surfaces is retained for long periods.[25] One method to activate polymers is known as plasma immersion ion implantation (PIII) in which ions from non-carbon-containing gases such as nitrogen, argon, or helium are accelerated under a high electric field to bombard polymer surfaces, producing a reservoir of radicals in the subsurface of the polymer (Figure 1a).[26] Another plasma activation method that can be used for more diverse substrates (polymers, metals, semiconductors, ceramics, or glass) is

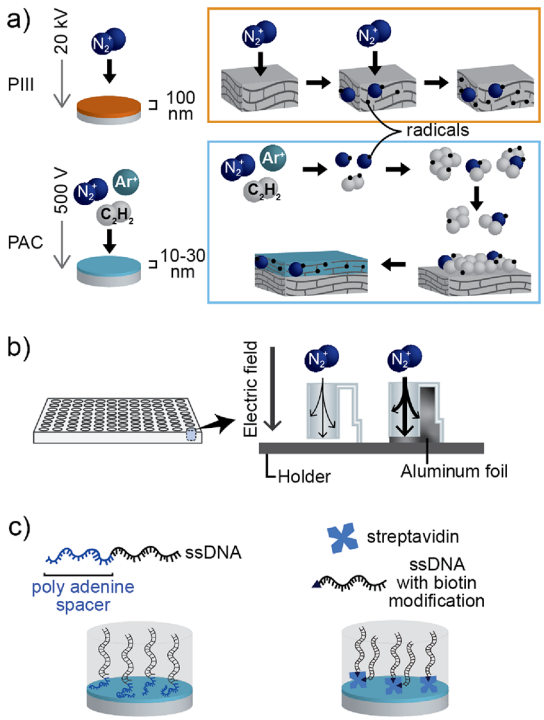

Figure 1. (a) Schematic of PIII and PAC treatments. (b) Microplate on the sample holder and addition of aluminum foil to improve conduction to the bottom of the microplate wells. (c) Immobilization of ssDNA and streptavidin to PIII- and PAC-treated microplates.

plasma-enhanced chemical vapor deposition (PECVD) combined with ion bombardment induced by substrate bias.[27] In this method, a mixture of gases including a carbon-containing gas is used to generate a plasma-activated coating (PAC) on the substrate surface.[24] Both PIII- and PAC-treated surfaces are rich in radicals that can form covalent bonds with biomolecules upon their contact with the surface. Proteins immobilized on PIII and PAC surfaces can form a dense monolayer, and their activity is retained.[26,28,29] Furthermore, DNA immobilized on PIII-treated polystyrene surfaces has been shown to hybridize with its complementary sequence strand.[30] However, PIII and PAC treatments of microplates have not been reported. Additionally, DNA immobilization on PAC surfaces has not been studied and PIII and PAC surfaces have not been directly compared for their surface properties and efficiency of biomolecule immobilization.

While PIII and PAC treatments have been demonstrated on flat substrates such as polymer sheets,[28,31] stainless steel,[29,32] and glass coverslips,[26] the effectiveness of these treatments on deep well structures such as microplates has not been explored. The deep walls of microplates have the potential to cause shadowing, preventing effective PIII or PAC treatment of the

https://doi.org/10.1021/acs.langmuir.2c02573
Langmuir 2023, 39, 343−356

well bottom. Existing plasma treatment strategies used to immobilize biomolecules on polystyrene microplates have drawbacks. For example, argon plasma activation has been used as a pretreatment for silane functionalization,[33] and nitrogen plasma activation has been used to introduce amine groups for functionalization with glutaraldehyde and other linkers.[34] However, these methods require further chemical activation steps and specific functional groups on the biomolecules. The density of active groups incorporated during plasma treatment in these approaches is also limited by gas mixtures required to produce a mechanically robust surface coating. Another approach involves the direct deposition of nebulized protein, such as collagen, on microplates by dielectric barrier discharge plasma.[35] However, this method requires large quantities of protein and not all biomolecules incorporated into the coating are accessible on the surface. PIII and PAC treatments for direct activation of microplates for biomolecule immobilization have the potential to mitigate these limitations.

In this study, we demonstrated PIII and PAC treatments activating 96-well polystyrene microplates for the immobilization of single-stranded DNA (ssDNA) and the protein streptavidin (Figure 1c). We select DNA to optimize the density and orientation of the immobilized molecules to achieve high hybridization densities.[9,36] Streptavidin is selected because it provides a generic linker for capture of any biotinylated molecule, including antibodies.[37] In addition, although the mechanisms of covalent binding of biomolecules in both PIII and PAC methods are based on the presence of radicals, each of these plasma activation techniques changes the physical and chemical properties of the substrates differently. These surface chemistry differences can potentially influence the density and orientation of adsorbed biomolecules on the surface prior to covalent bond formation. For the first time, we conducted a comprehensive comparison of the changes in optical properties, physical properties, and surface chemistry of microplates treated with different PAC recipes and PIII treatments. We then compared biomolecule immobilization on PAC and PIII to establish optimal protocols for DNA- and streptavidin-coated microplates and explored potential mechanisms behind covalent bond formation. Finally, we characterized the stability of PIII- and PAC-treated plates over 3 months. The results presented here demonstrate the potential of PIII- and PAC-treated microplates for a wide range of biological and biomedical assays and diagnostics.

EXPERIMENTAL SECTION

Microplate Preparation. Most commercially available microplates are tissue culture (TC)-treated, which is often described as some sort of a plasma treatment.[6] In this study, energetic ion plasma treatment was performed on TC-treated polystyrene (PS) microplates (CLS3603) (Sigma-Aldrich) and compared to unmodified TC-treated PS microplates and untreated (UT) PS microplates (CLS3370). These microplates have wells with a diameter of approximately 6 mm and a depth of approximately 11 mm. There is a 2−3 mm gap between the holder and the bottom of the well when the microplate is placed on either a PIII or a PAC stainless steel holder. Aluminum foil was molded to fill the gap in order to improve contact to the holder (Figure 1b). Microplates were cut into quarters with a hot wire cutter before plasma treatment, so they could be mounted on the sample holder in our small prototype plasma reactor and were taped back together for DNA and streptavidin immobilization and fluorescence detection.

PIII Treatment. PIII treatment was performed using inductively coupled radio frequency (RF) power at 13.56 MHz (ENI radio frequency power generator) to generate plasma, and a negative voltage bias was applied to a stainless-steel sample holder to accelerate positive ions toward the sample.[38] The pressure inside the chamber was evacuated to less than 5×10^{-5} Torr, and high-purity nitrogen gas was introduced and maintained at 2 mTorr during the treatment. The RF forwarded power was 100 W with a reverse power of 12 W when matched. Microplates, with or without aluminum foil, were taped on the stainless-steel holder with stainless steel mesh placed 5 cm from the holder and electronically connected to it. Nitrogen ions were accelerated through the mesh toward the stainless-steel holder with 20 kV negative bias pulses of 20 μs duration at a frequency of 50 Hz. The microplates were treated for 400 or 800 s (PIII-400 or PIII-800, respectively).

PAC Treatment. PAC treatment was performed in a separate plasma system using capacitively coupled RF power at 13.56 MHz (Eni OEM-6) and a negative pulsed bias generated by a RUP6 pulse generator (GBS Elektronik GmbH, Dresden, Germany).[39] Microplates with aluminum foil were positioned on a stainless-steel sample holder connected to RUP6, and the chamber was evacuated to less than 5×10^{-5} Torr. Prior to the plasma coating, microplates were activated with argon ions to facilitate coating adhesion for 2 min at an RF power of 75 W and an applied bias of 500 V. The pressure of argon inside the chamber was maintained around 7080 mTorr. For PAC deposition, a reactive gas mixture of acetylene, nitrogen, and argon was introduced into the chamber. The ratios between gases were controlled by setting flow rates on a mass flow controller (Allicat Scientific), and the pressure inside the chamber during the coating deposition was maintained at 110 mTorr. Plasma deposition was conducted with a plasma discharge of 50 W and a negative bias voltage of 500 V for 10 min. Negative bias from RUP 6 was applied with a frequency of 3 kHz and a pulse width of 20 μs. Four different gas ratios were chosen for comparison: no nitrogen, low nitrogen, moderate nitrogen, and high nitrogen (Table 2). Separate PAC treatments were performed on smooth silicon wafers with a native oxide layer to measure the coating thickness.

Table 2. PAC Treatments with Four Different Gas Flow Rate Recipes

	gas flow rate (SCCM)			
treatment	acetylene	nitrogen	argon	% nitrogen
no nitrogen	1	0	13	0
low nitrogen	1	3	10	21
mod nitrogen	1	10	3	71
high nitrogen	1	13	0	93

Upon exposure to air, radicals on the treated surfaces react with oxygen in the air to form oxygen-containing groups. These changes to the surface chemistry have been previously shown to saturate after a week.[40] Therefore, after each treatment, the microplates were covered in aluminum foil and stored for at least a week in air at room temperature before all subsequent analysis and biomolecule immobilization.

Ellipsometry. Ellipsometric spectroscopy was used to calculate the coating thickness of PAC deposited on silicon wafers. Ellipsometric data were collected at three angles of incidence (65°, 70°, and 75°) using a J.A Woollam M2000 V spectroscopic ellipsometer. A model consisting of a silicon substrate, silicon oxide layer (2 nm), and Cauchy layer to represent the PAC layer was used to fit the data in visible range to obtain the film thickness.

Water Contact Angle Measurements. The substrates were prepared by cutting out the bottom of the wells from the microplates and placing the surface under a mold, which is a 96-well microplate without the well bottoms for PIII and PAC treatments. The surface free energies of PIII- and PAC-treated, TC-treated 96-well microplates (1 week post treatment) were calculated and compared to

https://doi.org/10.1021/acs.langmuir.2c02573
Langmuir 2023, 39, 343−356

untreated polystyrene. Contact angle measurements using two liquid probes (water and diiodomethane) were performed using a Theta tensiometer (Biolin Scientific). Results were averaged over 10 drops for each sample. Surface free energies were calculated using the Owens−Wendt−Rabel−Kaelble method.

X-ray Photoelectron Spectroscopy. The compositions of elements present on PIII- and PAC-treated, TC-treated 96-well plates were determined by X-ray photoelectron spectroscopy (XPS, Thermo Fisher Scientific K-Alpha+) with a monochromated Al Kα X-ray source. Ten survey scans and five high-resolution scans of major elements (carbon, oxygen, nitrogen, and silicon) were taken on each sample for comparison. Element peak areas were divided by element-specific sensitivity factors and converted to atomic percentage for each element.

Electron Paramagnetic Resonance Spectroscopy. To measure radical densities, a polystyrene film (Goodfellow, thickness of 0.19 mm) was cut into 40 mm × 5 mm strips and treated with either PIII or PAC. The polystyrene film was used as a proxy for the microplate, which did not fit in the measurement instrument. The microwave absorption by unpaired electrons from the samples was measured using an electron paramagnetic resonance (EPR) spectrometer (Bruker EMX X-band). Measurements were done at room temperature with a microwave power of 2 mW and a frequency of 9.8 MHz. A magnetic field was scanned with a central value of 3523 G and a sweep width of 200 G. Ten scans were measured on each sample. A similar measurement was applied to 2,2diphenyl-1-picrylhydrazyl (DPPH) powder containing an EPR tube with known radical density to calculate the number of unpaired electrons on each sample.

Fourier Transform Infrared Attenuated Total Reflectance (FTIR-ATR) Spectroscopy. Changes in surface chemistry after plasma treatment were determined by comparison of the FTIR-ATR spectra of untreated and treated polystyrene prior to biomolecule immobilization. Polystyrene films were cut into small discs and placed at the bottom of microplate wells for PIII and PAC treatments. A week after the treatment, the discs were analyzed using a Hyperion FTIR spectrometer (Bruker) equipped with a micro germanium crystal ATR accessory. Each analysis consists of 128 scans with a resolution of 4 cm^{-1}. The spectra were normalized with the intensity of the 1490 cm^{-1} peak of polystyrene for comparison.

Absorbance and Autofluorescence Measurements. Changes in absorbance and autofluorescence after PIII and PAC treatments of microplates were measured with a PHERAstar FSX (BMG Labtech) and compared to untreated microplates. Absorbance was measured with the top optic at 450 nm with 22 flashes per well. Fluorescence intensity was measured at five commonly used excitation and emission wavelengths with five optic modules (460/510, 485/520, 540/580, 575/620, and 635-20/680-20). For each end point measurement, the top optic was used to scan the center of the well with 10 flashes, the focal height was adjusted for each sample, and the gain was set at 1400.

Immobilization of Single-Stranded DNA. The method for immobilization of single-stranded DNA (ssDNA) was based on previous work with PIII-treated polypropylene.[30] A 21-nucleotide (nt) ssDNA sequence (IDT DNA) was designed with a linker of 20 additional adenine nucleotides (Table 3). The 20 A linker had previously been shown to improve DNA attachment to plasma-treated surfaces with the correct orientation for DNA hybridization. It was expected that in acidic conditions, the amine groups in the adenine nucleotides of the linker will be protonated, and the linker will therefore be preferentially electrostatically attracted to the negatively charged plasma surface as compared to the core DNA sequence.

Table 3. Sequences of Immobilizing DNA, Hybridizing DNA, and Biotin DNA to Bind to Immobilized Streptavidin

DNA name	DNA sequence
immobilizing DNA	20xA-GCTCTGCAATCAACTTATCCC
hybridizing DNA	GGGATAAGTTGATTGCAGAGC-Alexa647
wrong hybridizing DNA	GTGATGTAGGTGGTAGAGGAA-Cy3
biotin DNA	biotin-GCTCTGCAATCAACTTATCCC

Wells of untreated and PIII- and PAC-treated 96-well microplates were incubated with 40 μL of 2 μM ssDNA in 10 mM citric acid/sodium citrate buffer at pH 3, 4, 5, or 6 or disodium hydrogen phosphate/sodium dihydrogen phosphate buffer at pH 7 or 8 for 1 h at room temperature on a shaker. DNA solution was replaced with 200 μL of 1% BSA in 10 mM PBS at pH 7.4 for 1 h at room temperature on a shaker to block the remaining active surface. BSA solution was removed, and the wells were washed three times with 200 μL of 2% SDS with vigorous shaking. After rinsing three times with 200 μL of Milli-Q water, DNA hybridization was performed by adding a 21 nt complementary DNA strand with 3′ Alexa647 fluorophore modification (IDT DNA; Table 3). Complementary DNA was added to a hybridization buffer (consisting of 2 mM magnesium chloride (Sigma-Aldrich), 1× Tris EDTA (Sigma-Aldrich), 1% BSA, and 0.6% SDS) to a final concentration of 0.8 μM. Each well was incubated with 40 μL of 0.8 μM complementary DNA solution for 1 h on a shaker at room temperature. The same hybridization process was repeated in a separate well for the noncomplementary DNA strand with a 3′ Cy3 fluorophore (Table 3). After removing the solution, the wells were washed three times with 200 μL of 10 mM PBS with vigorous shaking. Then, the wells were washed three times with vigorous shaking with 200 μL of each of three washing buffers: washing buffer 1 (2× saline-sodium citrate (SSC) + 0.6% SDS), washing buffer 2 (0.2× SSC + 0.6% SDS), and washing buffer 3 (0.1× SSC + 0.5% Tween 20). After rinsing the wells with 200 μL of 10 mM PBS, each well was filled with 40 μL of 10 mM PBS for fluorescence intensity measurement.

The fluorescence intensities of the Alexa647 and Cy3 modification on the complementary and noncomplementary DNA were measured with 635-20/680-20 and 540/580 optic modules on a PHERAstar FSX, respectively. For each measurement, the top optic was used to scan a 10 × 10 matrix with a well diameter of 3−5 mm with 10 flashes at each scan point. The focal height was adjusted for each sample, and the gain was set at 2000.

Immobilization of Streptavidin and Attachment of Biotin-DNA. Wells of plasma-treated and untreated microplates were incubated with 40 μL of 10 μg/mL streptavidin-Cy3 (Sigma-Aldrich, P6402) in 10 mM citric acid/sodium citrate buffer at pH 3, 4, 5, or 6 or disodium hydrogen phosphate/sodium dihydrogen phosphate buffer at pH 7 or 8 for 1 h at room temperature on a shaker. Streptavidin solution was replaced with 200 μL of 1% BSA in 10 mM PBS at pH 7.4 for 1 h at room temperature on a shaker to block the remaining active surface. BSA solution was removed, and the wells were rinsed three times with 200 μL of 10 mM PBS. After rinsing, each well was washed three times with 200 μL of 10% Triton in 10 mM PBS. Next, the wells were rinsed three times with 200 μL of 10 mM PBS, and then the wells were incubated with 2 μM 5′ biotin-modified ssDNA (IDT DNA; Table 3) in 10 mM PBS at pH 7.4 for 1 h at room temperature on a shaker. Following biotin-DNA incubation, the wells were incubated with the Alexa647-modified complementary DNA, as described in the DNA immobilization method. The hybridized surface was washed three times with 200 μL of washing buffer 4 (2× SSC + 0.05% Tween 20) before rinsing with 10 mM PBS. A PHERAstar FSX fluorescence plate reader with optic modules 540/580 and 635-20/680-20 was used to detect immobilized streptavidin-Cy3 and the hybridized complementary Alexa647-DNA, respectively. For each measurement, the top optic was used to scan a 10 × 10 matrix with a well diameter of 3−5 mm with 10 flashes at each scan point. The focal height was adjusted for each sample, and the gain was set at 1000.

RESULTS AND DISCUSSION

The amount of DNA or protein that can be usefully immobilized on a PIII or PAC microplate depends on the surface chemistry, optical properties, immobilization density, and orientation of biomolecules on the treated surface. PIII treatment introduces long-lived radicals into a modified surface

https://doi.org/10.1021/acs.langmuir.2c02573
Langmuir 2023, 39, 343−356

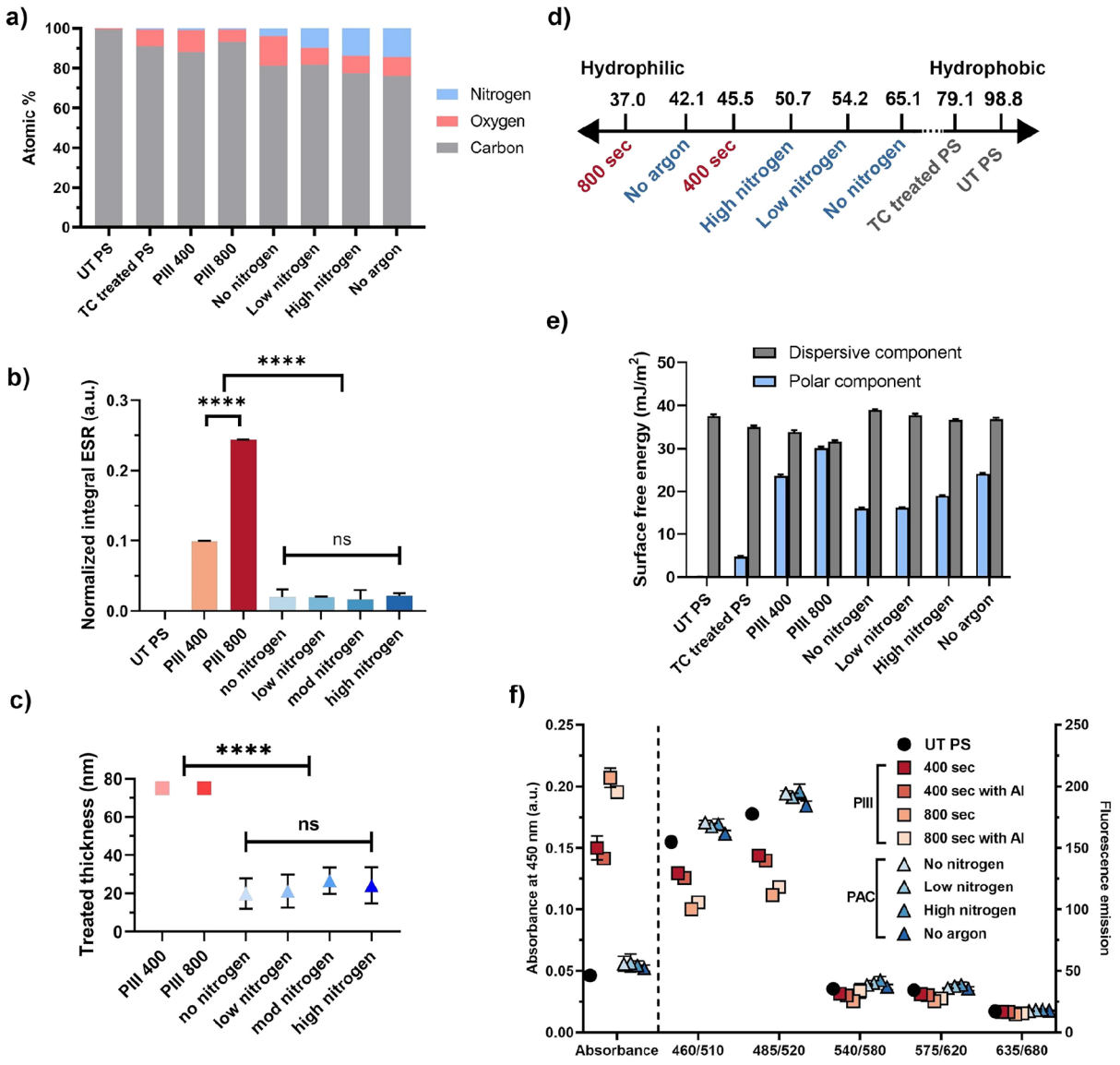

Figure 2. (a) Percentage surface elemental concentration of UT and TC-, PIII-, and PAC-treated PS microplates. (b) Comparison of relative electron paramagnetic resonance (EPR) integral intensity between UT and PIII- and PAC-treated PS. The measured EPR signal was integrated and normalized by the depth of radical penetration (PIII) or thickness of deposition layers (PAC). (c) Effective depth of the PIII treatment on polystyrene[38] and PAC thickness obtained from ellipsometry measurement of PAC-treated silicon wafers. (d) Water contact angles of UT and TC-, PIII-, and PAC-treated PS sheets placed in 96-well microplates during plasma treatment. (e) Dispersive and polar components of surface free energy of UT and TC-, PIII-, and PAC-treated PS microplates, calculated from the Owens−Wendt−Rabel−Kaelble method. The error bars represent their standard errors. (f) Mean absorbance and autofluorescence with SD of UT (circles) and PIII (squares)- and PAC (triangles)-treated PS microplates. SD bars are hidden when they are smaller than the marker size. The left column and *y* axis show absorbance at 450 nm, and the right column and *y* axis show the autofluorescence emission intensity at five excitation/emission wavelengths.

layer,[41,42] while PAC treatment deposits a polymer coating with a high concentration of long-lived radicals on surfaces.[43−45] PIII treatment leads to changes in nitrogen content,[26,38,41] while PAC results in deposition of a layer of hydrogenated amorphous carbon nitride from a mixture of acetylene and nitrogen gases,[45] and both surfaces undergo oxidation on exposure to air after treatment, leading to changes in oxygen content. Wettability, surface energy, optical absorbance, and autofluorescence are also known to be affected by PIII and PAC treatments.[26,29] To determine the optimal PIII and PAC treatment recipes for immobilized DNA and streptavidin microplates, the chemical properties of treated microplates were studied and then compared, including elemental composition, radical density, wettability, and surface energy. Optical absorbance and autofluorescence were similarly characterized and compared. Following this, the optimal treatment conditions were determined for high-density DNA and streptavidin immobilization on microplates. The hybridization efficiency of DNA-modified microplates and the biotin binding efficiency of streptavidin-modified microplates were determined to evaluate the useful binding capacity of the treated microplates.

Chemical Properties of PIII-Treated Microplates. The chemical composition of PIII-treated microplates was determined by XPS, comparing 400 s (PIII-400) and 800 s (PIII-800) treatment times (Figure 2a). The oxygen content of the PIII-treated microplates (6.1−11.1%) was not significantly different to the TC-treated microplates (8.3%). Similarly, the

https://doi.org/10.1021/acs.langmuir.2c02573
Langmuir 2023, 39, 343−356

surface nitrogen content was very low both before (0.6%) and after PIII treatment (0.5−0.8%). This was surprising as previous studies have shown an increase in nitrogen content (7−12%) following a 400 s PIII treatment of glass coverslips spin-coated with polystyrene[26] and an increase in oxygen composition from exposure to air following treatment of the polystyrene film.[40] Differences in the results observed here may be due to the deep well shape or differences in the type of polystyrene structure, such as the orientation of phenol groups, of the microplates as compared to the polystyrene film or spin-coated layers. The deconvolution of C 1s peaks is shown in the Supporting Information (Figure S1). The FTIR-ATR spectra did not show a noticeable difference between PIII-400 and PIII-800 (Figure S2).

Long-lived radicals appearing in the modified surface layer have been proposed as the main mechanism underlying covalent immobilization of biomolecules on PIII surfaces.[32] Radical densities of radicals in the samples can be calculated from EPR intensities by comparing with that obtained from a standard 2,2-diphenyl-1-picrylhydrazyl (DPPH) sample with known radical density. However, due to the difference in geometry and volume (DPPH powder was put in an EPR tube, while PIII- and PAC-treated PS strips were mounted on an EPR tube), we could not calculate the exact radical density on our samples. Instead, we compared the relative density of radicals in those samples by normalizing with the depth of the plasma treatment with the assumption that the measurement areas are the same for all samples.

For PIII samples, the depth of treatment was assumed to be 75 nm from the literature.[38] The relative density of radicals on treated microplates was found here to increase significantly (one-way ANOVA, $p < 0.0001$) after both 400 and 800 s PIII treatments (0.10 ± 0.001 and 0.24 ± 0.0003, respectively) compared to UT PS microplates (1.12×10^{-6}; Figure 2b and Figure S3). The increase from PIII-400 to PIII-800 was also significant (one-way ANOVA, $p < 0.0001$). These results agree with a previous study that has shown an increase in long-lived radical density with increasing PIII treatment time, which has been suggested to be due to an increased concentration of both dangling bonds and carbonized clusters that serve to stabilize the unpaired electrons in the radicals.[42]

The wettability of surfaces is another property known to be affected by PIII treatment. Here, PIII treatment was observed to significantly (one-way ANOVA, $p < 0.0001$) decrease the water contact angles of PIII-400 (45.5 ± 1.7°)- and PIII-800 (37.0 ± 1.9°)-treated microplates compared to TC-treated microplates (79.1 ± 0.6°) (Figure 2d). In contrast, previous studies found that water contact angles of PIII-treated flat substrates increased with treatment time.[26,40] The shape of the microplates may have contributed to this difference in trend. The Owens−Wendt−Rabel−Kaelble method considers the surface energy to be comprised of a polar component and a dispersive component. Polar components of PIII-treated microplates (23.7 ± 0.3 to 30.1 ± 0.3 mJ/m^2) were found to be significantly higher than TC-treated microplates (4.8 ± 0.1 mJ/m^2, one-way ANOVA, $p < 0.0001$) and increased with treatment time (Figure 2e). The wettability and polar surface energy component values for the PIII-treated microplates had a stronger correlation to the relative density of radicals as described above than to the surface nitrogen and oxygen composition, which agrees with previous findings.[46]

Chemical Properties of PAC-Treated Microplates. The chemical composition of PAC microplates was determined by XPS, comparing four different gas recipes containing increasing amounts of nitrogen: no nitrogen, low nitrogen, moderate (mod) nitrogen, and high nitrogen (Figure 2a and Figure S1). Surface nitrogen was found to increase with nitrogen content in the gas mixture across all PAC recipes. Values measured were TC (0.6%) and no-nitrogen (4.0%), low-nitrogen (9.7%), mod-nitrogen (13.8%), and high-nitrogen PAC (14.6%). For surface oxygen, no-nitrogen PAC-treated microplates had increased surface oxygen (14.9%). All other recipes had an oxygen content (8.5−9.4%) similar to that of TC-treated microplates (8.3%). It is important to note that the sampling depth measured by XPS (about 10 nm) may include the polystyrene substrate below the deposited layer, which would lower the nitrogen percentage. The nitrogen trend observed here agrees with observations made previously.[29] Other work has shown that deposited coatings can have as much as 35% nitrogen and 12.5% oxygen;[44] however, the use of a different substrate (stainless steel) prevents quantitative comparison of the results because the stainless steel composition can be removed from the calculation of atomic composition. The FTIR-ATR spectra did not show a significant difference between the four PAC recipes (Figure S2).

There was no significant difference between the relative density of radicals in different PAC-treated samples (Figure 2b; no nitrogen, 0.020 ± 0.01; low nitrogen, 0.019 ± 0.0008; mod nitrogen, 0.016 ± 0.013; high nitrogen, 0.021 ± 0.0035). As described above, these values were normalized with the PAC coating thickness (Figure 2c). The water contact angles of the microplates decreased after PAC treatment (Figure 2d). There was no significant difference in water contact angles between low- and mod-nitrogen PAC, but the hydrophilicity of high-nitrogen PAC was significantly higher than that of no-nitrogen PAC (one-way ANOVA, $p < 0.0001$). The water contact angles ranged between 42.1° and 65.1°. This trend is similar to previous findings with PAC-treated stainless steel.[29] The polar component of PAC samples also increased with increasing amount of nitrogen in the PAC recipe.

Comparison of Chemical Properties of PIII- and PAC-Modified Microplates. Overall, PIII microplates were found to have low surface nitrogen composition and high relative density of radicals and were very hydrophilic. PAC microplates had high nitrogen composition and moderate relative density of radicals and were more hydrophilic than untreated plates. PIII- and PAC-treated microplates were found to differ in several measured parameters. PAC-treated microplates had significantly higher amounts of surface nitrogen compared to PIII-treated microplates (PIII, 0.5−0.8%; PAC, 4−14.6%), while PIII-treated microplates had higher relative density of radicals (PIII, 0.10−0.24; PAC, 0.016−0.021) and were more hydrophilic (37.0−45.5°) compared to all PAC (50.7−65.1°) except the high nitrogen condition (42.1°). The relative density of radicals appeared to have a greater correlation with surface hydrophilicity than surface nitrogen and oxygen compositions.

Comparison of Optical Properties of PIII- and PAC-Modified Microplates. Changes in optical properties can impact the utility of plasma-activated microplates because optical readout is the main method of detection for biochemical plate assays. Thus, the effects of PIII and PAC treatments on absorbance and autofluorescence were characterized (Figure 2f). Absorbance was measured at 450 nm as this wavelength is used in many assays such as the HRP colorimetric assay.[27] The absorption spectra of PIII- and PAC-

https://doi.org/10.1021/acs.langmuir.2c02573
Langmuir 2023, 39, 343−356

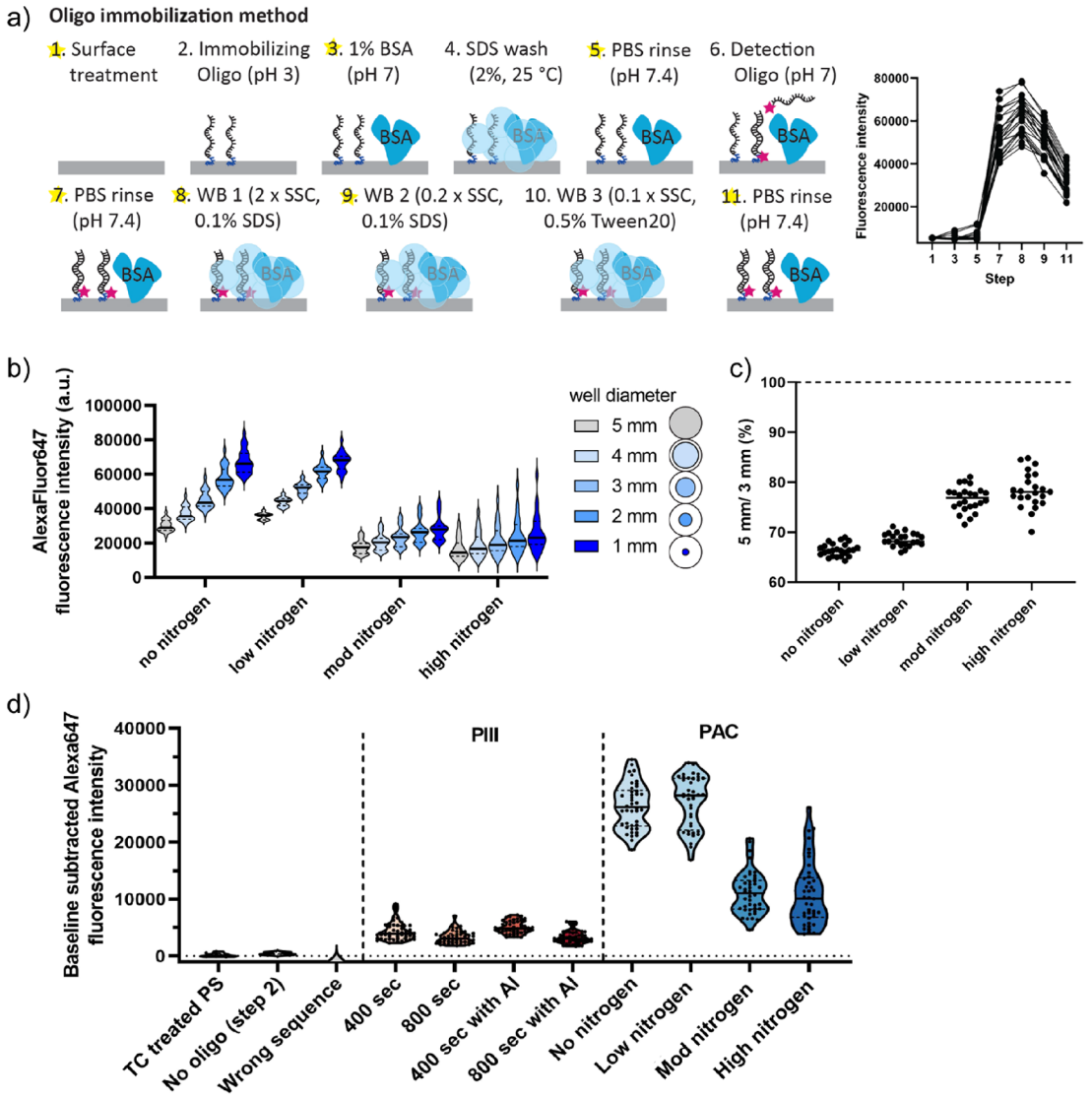

Figure 3. (a) Schematic diagram showing oligonucleotide immobilization methods and an example of data plotted on the graph on the right-hand side. The fluorescence intensity was measured at yellow-highlighted steps and shown on the graph. (b) Hybridized DNA distribution within the well on PAC-treated microplates. Fluorescence intensities were measured with well scan mode at a diameter of 1−5 mm within each well, and the average of each diameter is plotted in the graph. (c) Ratio of well average fluorescence intensity at 5 mm to the one at 3 mm. The dotted line at 100% represents a completely homogeneous density of DNA across the well area. (d) Baseline-subtracted Alexa647 fluorescence intensity of DNA immobilized (pH 4) and hybridized on TC-, PIII-, and PAC-treated microplates. The fluorescence spectra of immobilized DNA low-nitrogen PAC are shown in Figure S7.

treated microplates are shown in Figure S4. The mean absorbance at 450 nm was found to be significantly higher (one-way ANOVA, $p < 0.0001$) for PIII (0.150−0.207 a.u.) and PAC (0.052−0.056 a.u.) compared to untreated microplates (0.046 ± 0.001 a.u.). The greatest increase in the absorbance was observed for PIII-800 (0.207 ± 0.008 a.u.) followed by PIII-400 (0.150 ± 0.010 a.u.). Browning of the clear microplates by PIII treatment is in good agreement with previous observation that was explained from the formation of carbonized structures in the modified layer, which increase in number and size with longer treatment times.[26,47] PIII samples with aluminum had smaller variance in absorbance over multiple wells (0.016 a.u.) compared to the non-aluminum samples (0.030 a.u.), suggesting that the aluminum modification improved the uniformity of treatment across the microplate. PAC-treated microplates had a much smaller increase in absorbance (1.13- to 1.22-fold) compared to PIII-treated microplates (3.36- to 4.5-fold), with no significant difference between PAC gas recipes (0.052−0.056 a.u., one-way ANOVA, $p > 0.1$). It is known that PIII treatment causes deeper surface changes (75 nm) compared to PAC treatment (19.9−26.6 nm),[38] which may lead to the greater increase in optical absorbance observed here. Absorbance normalized by the treatment depth is shown in the Supporting Information (Figure S5). Overall, PIII resulted in a large (288%) increase in absorbance at 450 nm relative to the untreated microplate, while PAC had a more modest (17.5%) relative increase.

Generally, aromatic polymers have high autofluorescence at shorter wavelength due to low energy π to π^* transitions.[48] This agrees with the observations here, with all untreated and treated microplates having higher autofluorescence at shorter wavelengths (460/510 and 485/520 nm) than at longer wavelengths (540/580, 575/620, and 635/680 nm). In addition to this trend, PAC-treated microplates also had

https://doi.org/10.1021/acs.langmuir.2c02573
Langmuir 2023, 39, 343−356

significantly higher autofluorescence at shorter wavelengths (162−196, one-way ANOVA, $p < 0.0001$) compared to untreated microplates (155−157), while PIII-treated microplates had significantly lower autofluorescence (100−144, one-way ANOVA, $p < 0.0001$). Plasma treatment leads to the formation of highly conjugated double-bond structures and aromatic rings,[40] which may explain the increase in autofluorescence observed for PAC samples. In PIII treatment, heavy ion bombardment induces an amorphous carbon structure on the polymer surface, which explains the lower autofluorescence observed for PIII and supported by the observation that PIII-800 had lower autofluorescence (100−118) than PIII-400 (126−144). In contrast, at longer wavelengths, there is less difference in autofluorescence across all samples. Previously, PIII-800-treated PS-coated glass had been observed to have higher autofluorescence at a longer excitation wavelength (631 nm) compared to a shorter wavelength (488 nm).[26] However, optical measurements are a combination of surface and substrate properties, so differences in results here are likely due to substrate differences. Thus, overall PAC and PIII treatments changed microplate autofluorescence at shorter wavelengths (510−520 nm), but they had smaller changes at longer wavelengths (580−680 nm). The changes at shorter wavelengths were small relative to total autofluorescence from the polystyrene substrate, with PAC giving an 8% increase and PIII a 27% decrease. At longer wavelengths, PAC had a 9% increase and PIII had a 14% decrease from untreated polystyrene.

DNA Oligonucleotide Immobilization. For applications in DNA-binding assays, it is important for the immobilized DNA to maintain its ability to hybridize with complementary DNA. Therefore, measurements focused on the density of hybridized DNA, as detected by an Alexa647 fluorophore covalently attached to the hybridizing DNA oligonucleotide. The relative immobilized DNA density is shown in Figure S8. To correctly detect only DNA hybridized to covalently immobilized DNA, wash steps are required to remove nonspecifically bound DNA.[10] Wash steps were included to remove noncovalently bound ssDNA (step 4; Figure 3a) and nonhybridized ssDNA from the microplates (steps 7−11; Figure 3a). Wash methods selected were based on previous work[24,28,30] and were found to be effective at reducing the fluorescence signal of negative controls back to the baseline level (t-test, $p < 0.0001$) for both controls with no immobilizing ssDNA (step 2) or addition of the wrong sequence of hybridizing DNA (step 6; Figure 3c), for example, giving a 50% decrease from steps 7 to 11, which is equivalent to approximately 8.4×10^{10} DNA molecules removed from the surface. In preliminary measurements, the density of hybridized DNA was found to be higher in the center of the microplate wells compared to the edges (Figure 3b and Figure S6). Well edges are known to have less efficient fluid mixing[49] and experience a lower flux of implanting ions due to shadowing and the reduction of the sheath area-to-wall area ratio, which would limit the DNA density near the edge. Therefore, measurements of hybridization density were averaged over a circle with 3 mm diameter at the center of the wells, which had a total diameter of 5 mm.

We further quantified DNA distribution homogeneity by comparing an average over a circle with varying diameter at the center of the well to the total well area. The DNA density was found to be higher at the well center, with a trend of decreasing density away from the well center to the edges across all recipes (Figure 3b,c). However, the % change in density was found to be different between the four PAC recipes. DNA is hybridized more homogeneously across the well in moderate- and high-nitrogen PAC-treated wells (average signal across the well reduced by 22.5% on an increase in the area sampled). Therefore, these recipes would be suitable when more uniform and less crowded immobilized DNA surfaces are required. Low-nitrogen PAC-treated wells had overall higher DNA density compared to moderate- and high-nitrogen PAC-treated wells and better homogeneity of hybridized DNA compared to no-nitrogen PAC but less than moderate- or high-nitrogen PAC (average signal across the well reduced by 31.5% on the increase in the area sampled). When high-density immobilized DNA surfaces are required, low-nitrogen PAC-treated plates would be the best choice.

DNA hybridization was characterized for all recipes of PIII (PIII-400 and PIII-800) and PAC (no, low, mod, and high nitrogen). A greater fluorescence signal, indicating higher DNA hybridization density, was observed for all plasma-treated samples compared to the negative controls ($<3.1 \times 10^{10}$ molecules/cm^2) and was also higher on PAC-treated microplates than PIII-treated microplates (PIII, 1.3×10^{11} molecules/cm^2; PAC, 3.4×10^{11} molecules/cm^2; one-way ANOVA, $p < 0.0001$) (Figure 3c and Table 4). There was no

Table 4. Hybridized DNA and Immobilized Streptavidin Densities of TC, PIII, and PAC Microplates

surface modification	hybridization density ($\times 10^{11}$ molecules/cm^2)	SA density ($\times 10^{11}$ molecules/cm^2)
TC-treated	0.3	0.01
PIII-400	1.2	0.64
PIII-800	1.1	0.61
PIII-400 with Al	1.6	0.84
PIII-800 with Al	1.1	0.79
no nitrogen	4.8	2.2
low nitrogen	4.7	9.0
mod nitrogen	2.0	4.3
high nitrogen	2.0	4.0

hybridization when wrong sequence (noncomplementary) DNA was used, which indicates that the DNA is only binding through specific base-pairing. DNA hybridization was approximately 2- to 5-fold denser on PAC compared to PIII (1.1×10^{11} to 1.6×10^{11} molecules/cm^2, one-way ANOVA, $p < 0.0001$), and no- and low-nitrogen PAC recipes had the greatest amount of hybridized DNA overall (4.7×10^{11} to 4.8×10^{11} molecules/cm^2; one-way ANOVA, $p < 0.0001$). There was no significant difference between the four different PIII surfaces, indicating that the aluminum foil and treatment time did not affect DNA immobilization. The effect of pH on DNA immobilization was tested by incubating immobilizing ssDNA at pH 3−8 (step 2; Figure 3a). The highest hybridization density was observed for pH 3 and 4 for almost all PIII- and PAC-treated microplates (Figure 4a,b). The stability of plasma-treated plates over time before DNA immobilization and hybridization was also investigated. DNA immobilization capability of PIII-treated microplates decreased 1 month after the PIII treatment, but there was no further reduction up to 3 months (Figure 4c). All PAC samples retained the same DNA immobilization capability up to 3 months (Figure 4d). DNA immobilization and hybridization on no- and low-nitrogen

https://doi.org/10.1021/acs.langmuir.2c02573
Langmuir 2023, 39, 343−356

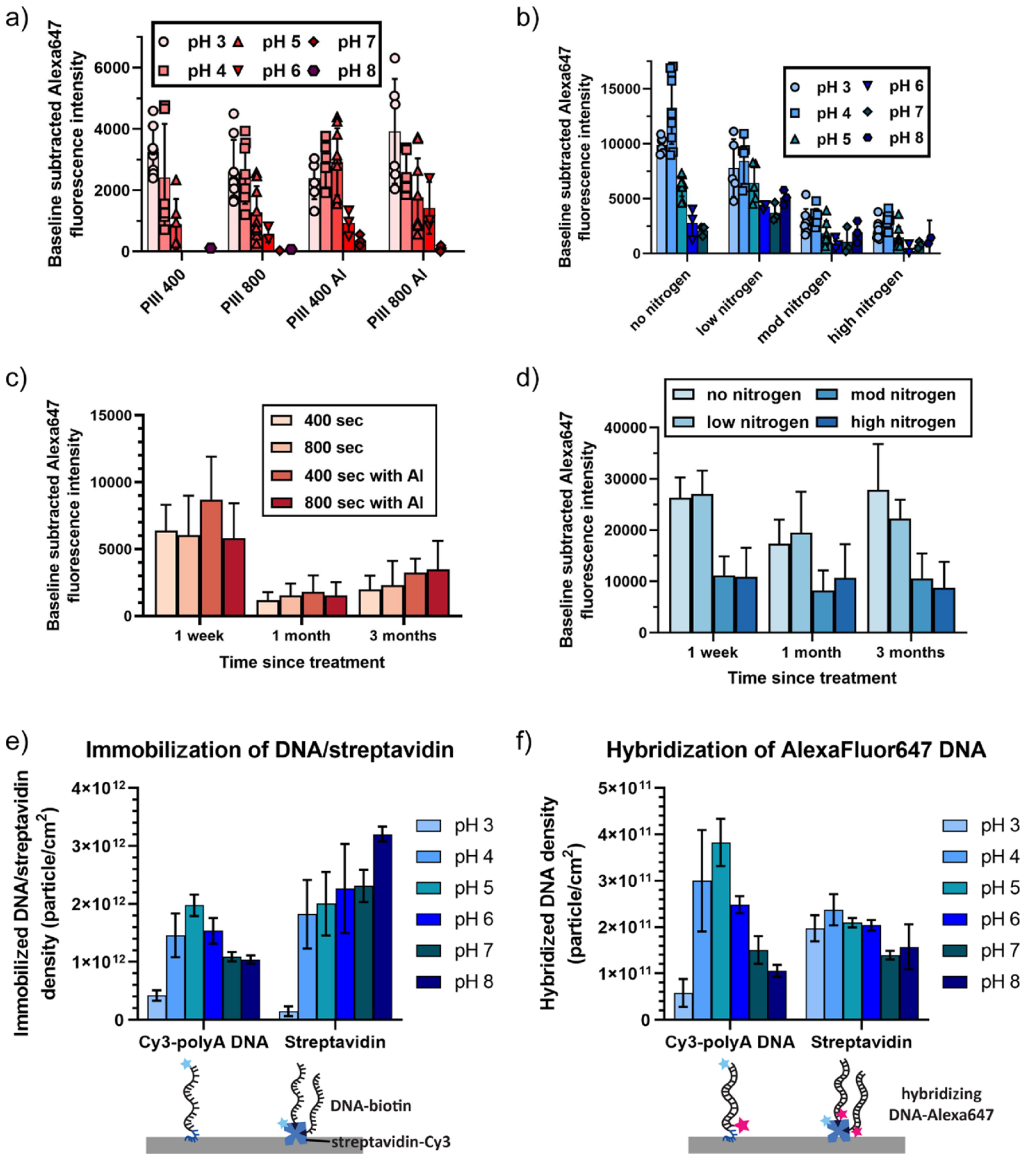

Figure 4. (a) DNA immobilization and hybridization on PIII-treated microplates at pH 3−8. (b) DNA immobilization and hybridization on PAC-treated microplates at pH 3−8. (c) DNA immobilization and hybridization to PIII-treated microplates 1 week, 1 month, and 3 months after treatment. (d) DNA immobilization and hybridization to PAC-treated microplates 1 week, 1 month, and 3 months after treatment. PAC-treated plates were stored at room temperature for 1 week, 1 month, or 3 months before DNA immobilization and hybridization. (e) Immobilized DNA and streptavidin density on a low-nitrogen PAC-treated 384-well microplate at pH 3−8. (f) Hybridized AlexaFluor647 DNA density on immobilized DNA and streptavidin low-nitrogen PAC-treated 384-well microplates (pH refers to immobilization pH).

PAC samples were further optimized by using freshly prepared hybridization solution and measuring fluorescence intensity from the 3 mm diameter instead of the 5 mm diameter. After further optimization, the average hybridized density on no-nitrogen and low-nitrogen PAC increased to 5.2×10^{12} molecules/cm^2 (Figure S9).

Low-nitrogen PAC treatment was also applied to 384-well microplates (PerkinElmer, OptiPlate-384 black) for immobilization of DNA and streptavidin (Figure 4e). DNA and streptavidin immobilized at high densities on the low-nitrogen PAC-treated 384-well microplates (2×10^{12} and 3.2×10^{12} molecules/cm^2, respectively). The hybridization densities of AlexaFluor647 DNA on the 384-well microplates were similar to the results from 96-well microplates (Figure 4f, 2.4×10^{11} to 3.8×10^{11} molecules/cm^2).

Interestingly, the measured relative density of radicals was found not to correlate with the amount of DNA hybridized to the surface. PIII microplates had a 5- to 15-fold higher relative density of radicals than PAC but a 2- to 5-fold lower DNA hybridization capacity. This demonstrates that the low amount of radicals on PAC surfaces was sufficient for dense DNA immobilization. Previously, it was reported that electrostatic and hydrophobic forces played important roles in immobilization of yeast cells on PIII-treated surfaces.[50] Similarly, here, we found stronger correlations between the surface charge and the hydrophobicity of treated surfaces and the amount of immobilized and hybridized DNA.

Intermolecular interactions between DNA and the surface are important because the DNA needs to come close to the surface to react with the radicals and form covalent bonds. DNA adsorption to surfaces is impacted by long-range

https://doi.org/10.1021/acs.langmuir.2c02573
Langmuir 2023, 39, 343−356

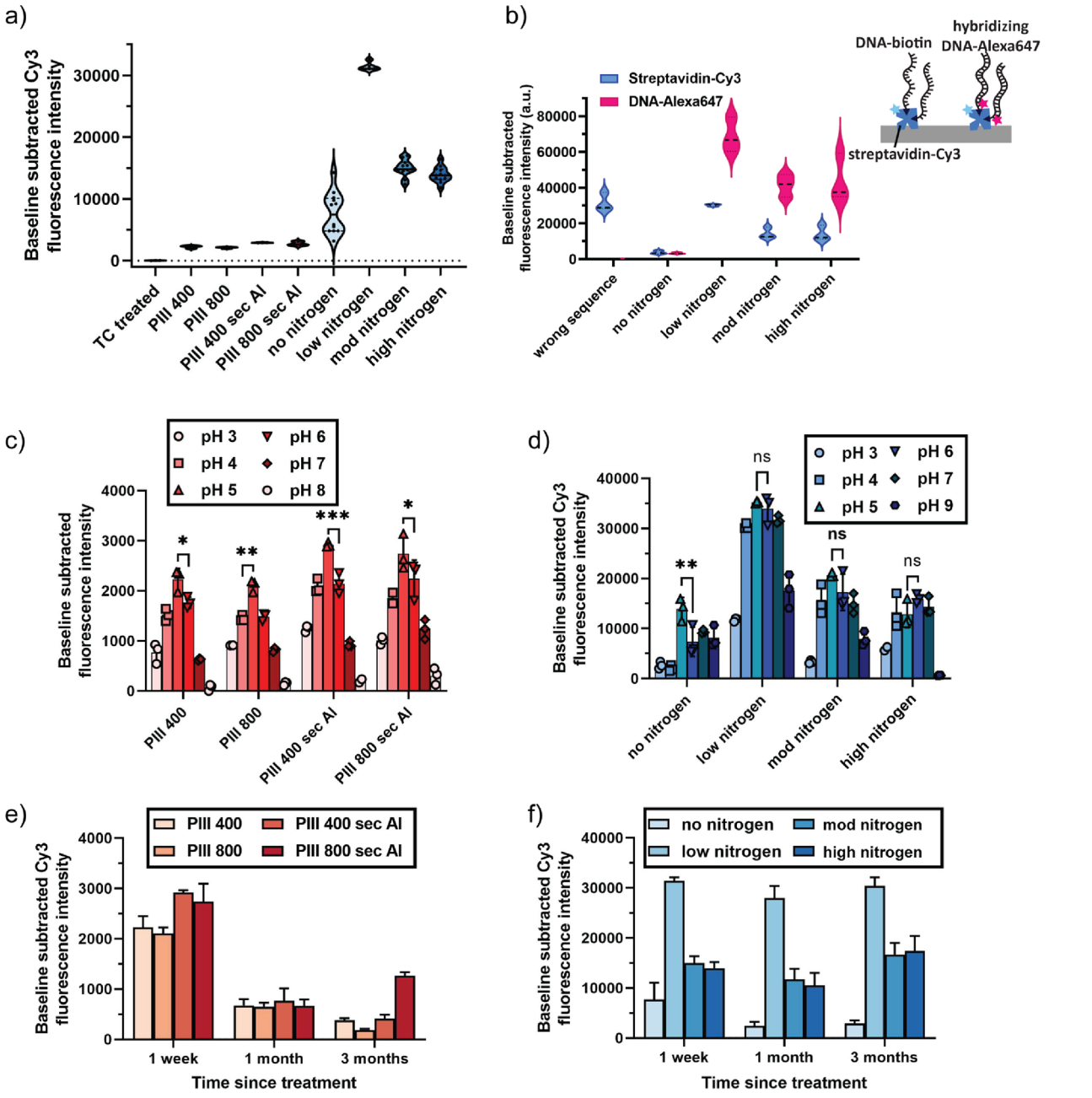

Figure 5. Streptavidin immobilization to microplates. (a) Cy3 fluorescence intensity of streptavidin-Cy3 immobilized on TC-, PIII-, and PAC-treated microplates. (b) Ability of immobilized streptavidin to bind with biotin. (c) Streptavidin immobilization to PIII-treated microplates at pH 3−8. (d) Streptavidin immobilization to PAC-treated microplates at pH 3−9. (e) Streptavidin immobilization to 1 week-, 1 month-, and 3 month-old PIII-treated microplates. (f) Streptavidin immobilization to 1 week-, 1 month-, and 3 month-old PAC-treated microplates. The fluorescence spectra of immobilized streptavidin low-nitrogen PAC are shown in Figure S7.

electrostatic forces and short-range forces such as van der Waals (vdW).[51] Plasma-treated surfaces are known to be negatively charged at higher pH and more neutrally charged at lower pH.[50] At neutral pH, each phosphate group on the DNA backbone has a negative charge with a $pK_a < 2$, and all bases are neutrally charged.[52] Therefore, it is expected that there will be an electrostatic repulsion between the surface and DNA at neutral pH, which scales with $1/r^2$, where r is the distance between the two species.[51,53] By using lower pH during immobilization, the DNA density improved significantly. At lower pH, it is expected that surface nitrogen and oxygen groups are protonated and become less negatively charged.[50] Similarly, nucleobases adenine and cytosine are also expected to be protonated (pK_a = 3.52 and 4.17, respectively),[52] and thus, the polyadenine spacer on the immobilizing DNA strand will become less negatively charged.[50,51] Note that DNA has good stability at pH 3 for at least 1 h, which is the condition used here for DNA immobilization, but that depurination can occur at lower pH.[51] PAC surfaces had higher DNA density than PIII surfaces, which could be explained by the higher composition of nitrogen that could be protonated on PAC surfaces, leading to more favorable electrostatic interactions. However, the highest DNA density was found on PAC surfaces

https://doi.org/10.1021/acs.langmuir.2c02573
Langmuir 2023, 39, 343−356

with lower composition of surface nitrogen. Thus, charge interactions cannot fully explain the results observed.

The hydrophilicity of the surface is another important factor that could affect the intermolecular interaction with DNA. Both hydrophilic and hydrophobic surfaces can attract DNA.[53] Hydrophobic surfaces can attract nearby DNA through short-range vdW forces, and hydrophilic surfaces can attract longer-range DNA via dipole−dipole and hydrogen bonding. However, hydrophilic surfaces are more susceptible to form a dense hydration layer, which competes with intermolecular attraction between the surface and DNA via hydrogen bonding. Thus, higher DNA density on the no- and low-nitrogen PAC surfaces compared to other samples could be explained by their relative hydrophobicity compared to mod- and high-nitrogen PAC and all PIII conditions, which minimizes the formation of the hydration layer and maximizes vdW forces.

Streptavidin Immobilization. Streptavidin immobilized on plasma-treated surfaces was directly detected by the fluorescence of covalently modified Cy3 streptavidin. For PAC surfaces, it was also indirectly detected by binding with dual biotin-modified Alexa647-modified DNA strands. While the former quantifies protein immobilized, the latter will only detect active protein on the surface. Similar to DNA, streptavidin was also found to bind more on PAC-treated microplates than PIII-treated microplates (Figure 5a), with a significant increase for all plasma-treated conditions above the nontreated control (TC-treated, 0.01×10^{11} molecules/cm^2; PIII, 0.7×10^{11} molecules/cm^2; PAC, 4.9×10^{11} molecules/cm^2; one-way ANOVA, $p < 0.0001$). In contrast to DNA, low-nitrogen PAC had the highest amount of bound streptavidin (no nitrogen, 2.2×10^{11} molecules/cm^2; low nitrogen, 9.0×10^{11} molecules/cm^2; mod nitrogen, 4.3×10^{11} molecules/cm^2; high nitrogen, 4.0×10^{11} molecules/cm^2), whereas DNA immobilizations on both low- and no-nitrogen PAC were similar. This trend observed on PAC surfaces was reproduced for biotin-DNA binding, indicating that the immobilized protein remains available for biotin binding (Figure 5b; no nitrogen, 0.6×10^{11} molecules/cm^2; low nitrogen, 12.2×10^{11} molecules/cm^2; mod nitrogen, 7.3×10^{11} molecules/cm^2; high nitrogen, 7.8×10^{11} biotin-DNA molecules/cm^2). There was no DNA hybridization to bound biotin-DNA when wrong sequence DNA was used. By calculation, there was an average of 2.14 hybridized DNA-biotin molecules bound to each immobilized streptavidin on the surface. The best PIII surface for streptavidin immobilization was PIII-400 with aluminum, but it had about 10-fold less streptavidin compared to the best PAC condition. The pH of immobilization buffers influenced the amount of immobilized streptavidin on PIII and PAC microplates. For PIII microplates, the optimum immobilization was achieved at pH 5 (Figure 5c). For PAC microplates, optimum streptavidin immobilization was achieved at pH 5 for no-nitrogen PAC and at pH 4−7 for the other PAC recipes (Figure 5d). The stability of PIII-treated microplates deteriorated significantly after 1 month as reflected by its ability to immobilize streptavidin (Figure 5e). However, the ability to immobilize streptavidin did not change significantly for PAC samples up to 3 months old (Figure 5f).

These results suggest that the immobilization of streptavidin to PIII and PAC surfaces is also dominated by electrostatic interactions and surface hydrophilicity. Streptavidin has a pI of 5, which matches with the optimum immobilization pH found on both PIII and PAC surfaces. This indicates that neutrally charged streptavidin is favorable for immobilization. Zero charge on the protein may result in better packing of protein on the surface as it eliminates repulsion between protein molecules as they arrive on the surface. This phenomenon is very interesting and needs further investigation with other proteins to study their optimum immobilization pH. Streptavidin is very hydrophilic, and it is known to be more attracted to hydrophilic surfaces.[54] However, it did not bind well to PIII-treated surfaces, even though they were the most hydrophilic surfaces of all. Again, it could be that on very hydrophilic PIII and PAC surfaces, there is a dense hydration layer, which limits streptavidin binding on more hydrophilic surfaces. Low-nitrogen PAC surfaces may have a good balance between hydrophobicity and hydrophilicity, which minimizes competition with water. However, further investigation of the surface properties is required to confirm these proposed mechanisms.

Summary of Optimized Conditions. PIII and PAC plasma treatments of 96-well polystyrene microplates resulted in covalently immobilized DNA and streptavidin in a single step without the use of linkers. High-density DNA immobilization was achieved on no- and low-nitrogen PAC at pH 3−4. Streptavidin immobilization was optimal on low-nitrogen PAC-treated microplates at pH 5−7. These PAC-treated microplates remained active for the immobilization for at least 3 months. The maximum hybridized DNA density obtained with no- and low-nitrogen PAC was about 5.2×10^{12} molecules/cm^2, which is similar to the values reported in studies that use chemically activated surfaces to covalently immobilize DNA[55,56] (Table 1). PAC treatment simplifies the microplate functionalization process and eliminates risks associated with additional reagents. The current process time to modify microplates with plasma treatment takes 15 min, which does not include evacuation and venting time. A scaled-up plasma system will allow multiple plates to be treated at a time and therefore reduce the manufacturing time and cost.

Despite these benefits, the exact mechanism for covalent immobilization of biomolecules to plasma-treated surfaces is still not fully characterized. This makes it difficult to predict the best conditions for new applications with different biomolecules. While the surface biomolecule density did not correlate with radical density, it was observed to be affected by surface nitrogen composition, charge interactions, and hydrophilicity. For new applications, optimization of immobilization conditions, such as pH and PAC gas mixture, would still be required. In the future, it could be useful to create a library of reference proteins with different pI values to help estimate the optimal immobilization pH. Also, PAC surfaces were found to have slightly higher background fluorescence at lower wavelength (8% increase from UT surfaces), which is important to consider for selection of compatible fluorophores for optical detection. Currently, plasma-treated microplates remain stable up to 3 months; however, the long-term stability of the DNA- and streptavidin-coated microplates is not known and requires further characterization.

CONCLUSIONS

PAC surfaces were found to have more nitrogen and lower radical density and were more hydrophobic and more stable over 3 months than PIII surfaces. Optimal conditions were obtained for high-density DNA (PAC, 0 or 21% nitrogen, pH 3−4) and streptavidin (PAC, 21% nitrogen, pH 5−7) binding. DNA hybridization and protein activity of immobilized

https://doi.org/10.1021/acs.langmuir.2c02573
Langmuir 2023, 39, 343−356

molecules were confirmed on 96- and 384-well plates. We show that PAC-activated microplates allow for high-density covalent immobilization of functional DNA and protein in a single step without specific linker chemistry.

Immobilized PAC biomolecule microplates could be used for a range of new applications, for example, DNA-based assays such as solid phase polymerase chain reaction (PCR) to capture complementary DNA from clinical samples for PCR reactions. The sequence of the DNA can be altered as long as it has a 20-adenine tail. Immobilized streptavidin microplates could be used to tether any molecules with biotin modifications. Additionally, other biomolecules could be immobilized on PAC-treated microplates without using any additional linkers. For example, PAC-treated microplates could be coated with avidin or antibody binding proteins, and then colorimetric or fluorescence assays could be performed for the detection of biomolecules. Alternatively, PAC-treated microplates could be used as a cell culture platform by attaching extracellular matrix proteins to support cell culture. For example, previous studies showed that the tropoelastin immobilized PAC surface enhanced endothelial cell growth up to 5 days,[29] and the fibronectin immobilized PAC surface enhanced primary osteoblast growth up to 14 days.[45] Future extension of this method to even higher throughput plate formats, such as 1536-well plates, also has the potential to facilitate high-throughput screening (HTS) assays in drug development. However, edge effects could potentially decrease the homogeneity of biomolecule immobilization across the well on higher throughput plates and would need further optimization. Ultimately, plasma activation of microplates will allow for a faster and more convenient platform to study biological processes with user-selected biomolecules.

■ ASSOCIATED CONTENT

Supporting Information

The Supporting Information is available free of charge at https://pubs.acs.org/doi/10.1021/acs.langmuir.2c02573.

Additional data including deconvolution of C 1s peaks of PIII/PAC-treated microplates, FTIR-ATR of PIII/PAC-treated microplates, EPR spectrum of PIII/PAC-treated PS sheets, absorbance spectra of PIII/PAC-treated microplates, normalized absorbance of PIII/PAC-treated microplates, fluorescence spectra of low-nitrogen PAC, immobilized DNA low-nitrogen PAC and immobilized streptavidin low-nitrogen PAC, relative immobilized DNA density, and further optimized DNA hybridization results (PDF)

■ AUTHOR INFORMATION

Corresponding Authors

Clara T. H. Tran − *School of Physics, The University of Sydney, Sydney, NSW 2006, Australia*; Email: clara.tran@sydney.edu.au

Anna Waterhouse − *School of Medical Sciences, The University of Sydney Nano Institute, and Charles Perkins Centre, The University of Sydney, Sydney, NSW 2006, Australia; The Heart Research Institute, The University of Sydney, Newtown 2042, Australia;* orcid.org/0000-0003-1498-9393; Email: anna.waterhouse@sydney.edu.au

Shelley F. J. Wickham − *School of Chemistry, School of Physics, and The University of Sydney Nano Institute, The University of Sydney, Sydney, NSW 2006, Australia;* orcid.org/0000-0002-5658-3546; Phone: +61 29351 3366; Email: shelley.wickham@sydney.edu.au

Authors

Kanako Coffi Dit Gleize − *School of Chemistry, The University of Sydney, Sydney, NSW 2006, Australia*

Marcela M. M. Bilek − *School of Physics, The University of Sydney Nano Institute, Charles Perkins Centre, and School of Biomedical Engineering, Faculty of Engineering, The University of Sydney, Sydney, NSW 2006, Australia;* orcid.org/0000-0003-3363-2664

Complete contact information is available at: https://pubs.acs.org/10.1021/acs.langmuir.2c02573

Notes

The authors declare the following competing financial interest(s): K.C.D.G, C.T. H.T, M.B. and S.W. are inventors of a provisional patent relevant to this work (Australian application no. 2022902232) filed by Ionised Technologies Pty Ltd, and are shareholders of the company. Other authors have no conflict of interest to declare.

■ ACKNOWLEDGMENTS

The authors thank Dr. Jonathan Berengut and Dr. Stuart Fraser for helpful discussion. XPS measurements were carried out by Sydney Analytical at The University of Sydney. We acknowledge funding from the Australian Research Council (ARC) (DE180101635 (S.F.J.W.) and FL190100216 (M.M.M.B.)), Westpac Research Fellowship (S.F.J.W. and K.C.D.G.), The University of Sydney, The Heart Research Institute, and The University of Sydney Nano Institute.

■ REFERENCES

(1) Butler, J. E. Solid Supports in Enzyme-Linked Immunosorbent Assay and Other Solid-Phase Immunoassays. *Methods* **2000**, *22*, 4−23.

(2) Engvall, E.; Perlmann, P. Enzyme-linked immunosorbent assay (ELISA) quantitative assay of immunoglobulin G. *Immunochemistry* **1971**, *8*, 871−874.

(3) Lequin, R. M. Enzyme immunoassay (EIA)/enzyme-linked immunosorbent assay (ELISA). *Clin. Chem.* **2005**, *51*, 2415−2418.

(4) Zhang, Z.-R.; Hughes, M. D.; Morgan, L. J.; Santos, A. F.; Hine, A. V. *Fluorescent microplate-based analysis of protein-DNA interactions II: immobilized DNA*. 2018, *35*(5), 988-996; DOI: 10.2144/03355st07

(5) Desbordes, S. C.; Studer, L. Adapting human pluripotent stem cells to high-throughput and high-content screening. *Nat. Protoc.* **2013**, *8*, 111−130.

(6) Barker, S. L.; LaRocca, P. J. Method of production and control of a commercial tissue culture surface. *J. Tissue Cult. Methods* **1994**, *16*, 151−153.

(7) Gharaibeh, B.; Lu, A.; Tebbets, J.; Zheng, B.; Feduska, J.; Crisan, M.; Peault, B.; Cummins, J.; Huard, J. Isolation of a slowly adhering cell fraction containing stem cells from murine skeletal muscle by the preplate technique. *Nat. Protoc.* **2008**, *3*, 1501−1509.

(8) Nagaoka, M.; Koshimizu, U.; Yuasa, S.; Hattori, F.; Chen, H.; Tanaka, T.; Okabe, M.; Fukuda, K.; Akaike, T. E-Cadherin-Coated Plates Maintain Pluripotent ES Cells without Colony Formation. *PLoS One* **2006**, *1*, No. e15.

(9) Nimse, S.; Song, K.; Sonawane, M.; Sayyed, D.; Kim, T. Immobilization Techniques for Microarray: Challenges and Applications. *Sensors* **2014**, *14*, 22208−22229.

(10) Dugas, V.; Depret, G.; Chevalier, Y.; Nesme, X.; Souteyrand, E. Immobilization of singlestranded DNA fragments to solid surfaces and their repeatable specific hybridization: covalent binding or adsorption? *Sens. Actuators, B* **2004**, *101*, 112−121.

(11) Butler, J. E.; Ni, L.; Brown, W. R.; Joshi, K. S.; Chang, J.; Rosenberg, B.; Voss, E. W., Jr. The immunochemistry of sandwich elisas—VI. Greater than 90% of monoclonal and 75% of polyclonal anti-fluorescyl capture antibodies (CAbs) are denatured by passive adsorption. *Mol. Immunol.* **1993**, *30*, 1165−1175.
(12) Yousefi, H.; Su, H.-M.; Ali, M.; Filipe, C. D. M.; Didar, T. F. Producing Covalent Microarrays of Amine-Conjugated DNA Probes on Various Functional Surfaces to Create Stable and Reliable Biosensors. *Adv. Mater. Interfaces* **2018**, *5*, 1800659.
(13) Vroman, L.; Adams, A. L. Findings with the recording ellipsometer suggesting rapid exchange of specific plasma proteins at liquid/solid interfaces. *Surf. Sci.* **1969**, *16*, 438−446.
(14) Kaur, J.; Singh, K. V.; Raje, M.; Varshney, G. C.; Suri, C. R. Strategies for direct attachment of hapten to a polystyrene support for applications in enzyme-linked immunosorbent assay (ELISA). *Anal. Chim. Acta* **2004**, *506*, 133−135.
(15) Chrisey, L. Covalent attachment of synthetic DNA to self-assembled monolayer films. *Nucleic Acids Res.* **1996**, *24*, 3031−3039.
(16) Rogers, Y.-H.; Jiang-Baucom, P.; Huang, Z.-J.; Bogdanov, V.; Anderson, S.; Boyce-Jacino, M. T. Immobilization of Oligonucleotides onto a Glass Support via Disulfide Bonds: A Method for Preparation of DNA Microarrays. *Anal. Biochem.* **1999**, *266*, 23−30.
(17) O'Donnell, M. J.; Tang, K.; Köster, H.; Smith, C. L.; Cantor, C. R. High-Density, Covalent Attachment of DNA to Silicon Wafers for Analysis by MALDI-TOF Mass Spectrometry. *Anal. Chem.* **1997**, *69*, 2438−2443.
(18) Rehman, F. N.; Audeh, M.; Abrams, E. S.; Hammond, P. W.; Kenney, M.; Boles, T. C. Immobilization of acrylamide-modified oligonucleotides by co-polymerization. *Nucleic Acids Res.* **1999**, *27*, 649−655.
(19) Zhang, Y.; Li, L.; Yu, C.; Hei, T. Chitosan-coated polystyrene microplate for covalent immobilization of enzyme. *Anal. Bioanal. Chem.* **2011**, *401*, 2311−2317.
(20) Hoffmann, C.; Pinelo, M.; Woodley, J. M.; Daugaard, A. E. Development of a thiol-ene based screening platform for enzyme immobilization demonstrated using horseradish peroxidase. *Biotechnol. Prog.* **2017**, *33*, 1267−1277.
(21) Jeon, B.-J.; Kim, M.-H.; Pyun, J.-C. Parylene-A coated microplate for covalent immobilization of proteins and peptides. *J. Immunol. Methods* **2010**, *353*, 44−48.
(22) Yoo, G.; Park, M.; Lee, E.-H.; Jose, J.; Pyun, J.-C. Immobilization of E. coli with autodisplayed Z-domains to a surface-modified microplate for immunoassay. *Anal. Chim. Acta* **2011**, *707*, 142−147.
(23) Wang, S.; Wen, S.; Shen, M.; Guo, R.; Cao, X.; Wang, J.; Shi, X. Aminopropyltriethoxysilane-mediated surface functionalization of hydroxyapatite nanoparticles: synthesis, characterization, and in vitro toxicity assay. *Int. J. Nanomed.* **2011**, *6*, 3449−3459.
(24) Bilek, M. M.; McKenzie, D. R. Plasma modified surfaces for covalent immobilization of functional biomolecules in the absence of chemical linkers: towards better biosensors and a new generation of medical implants. *Biophys. Rev.* **2010**, *2*, 55−65.
(25) Nosworthy, N. J.; Ho, J. P. Y.; Kondyurin, A.; McKenzie, D. R.; Bilek, M. M. M. The attachment of catalase and poly-l-lysine to plasma immersion ion implantation-treated polyethylene. *Acta Biomater.* **2007**, *3*, 695−704.
(26) Kosobrodova, E.; Gan, W. J.; Kondyurin, A.; Thorn, P.; Bilek, M. M. M. Improved Multiprotein Microcontact Printing on Plasma Immersion Ion Implanted Polystyrene. *ACS Appl. Mater. Interfaces* **2018**, *10*, 227−237.
(27) Yin, Y.; Fisher, K.; Nosworthy, N. J.; Bax, D.; Rubanov, S.; Gong, B.; Weiss, A. S.; McKenzie, D. R.; Bilek, M. M. M. Covalently Bound Biomimetic Layers on Plasma Polymers with Graded Metallic Interfaces for in vivo Implants. *Plasma Processes Polym.* **2009**, *6*, 658−666.
(28) Gan, B. K.; Kondyurin, A.; Bilek, M. M. M. Comparison of protein surface attachment on untreated and plasma immersion ion implantation treated polystyrene: protein islands and carpet. *Langmuir* **2007**, *23*, 2741−2746.
(29) Waterhouse, A.; Yin, Y.; Wise, S. G.; Bax, D. V.; McKenzie, D. R.; Bilek, M. M. M.; Weiss, A. S.; Ng, M. K. C. The immobilization of recombinant human tropoelastin on metals using a plasma-activated coating to improve the biocompatibility of coronary stents. *Biomaterials* **2010**, *31*, 8332−8340.
(30) Tran, C. T. H.; Craggs, M.; Smith, L. M.; Stanley, K.; Kondyurin, A.; Bilek, M. M.; McKenzie, D. R. Covalent linker-free immobilization of conjugatable oligonucleotides on polypropylene surfaces. *RSC Adv.* **2016**, *6*, 83328−83336.
(31) Kosobrodova, E.; Mohamed, A.; Su, Y.; Kondyurin, A.; dos Remedios, C. G.; McKenzie, D. R.; Bilek, M. M. M. Cluster of differentiation antibody microarrays on plasma immersion ion implanted polycarbonate. *Mater. Sci. Eng., C* **2014**, *35*, 434−440.
(32) Bilek, M. M. M.; Bax, D. V.; Kondyurin, A.; Yin, Y.; Nosworthy, N. J.; Fisher, K.; Waterhouse, A.; Weiss, A. S.; dos Remedios, C. G.; McKenzie, D. R. Free radical functionalization of surfaces to prevent adverse responses to biomedical devices. *Proc. Natl. Acad. Sci. U. S. A.* **2011**, *108*, 14405−14410.
(33) North, S. H.; Lock, E. H.; Cooper, C. J.; Franek, J. B.; Taitt, C. R.; Walton, S. G. Plasma-Based Surface Modification of Polystyrene Microtiter Plates for Covalent Immobilization of Biomolecules. *ACS Appl. Mater. Interfaces* **2010**, *2*, 2884−2891.
(34) Boulares-Pender, A.; Prager-Duschke, A.; Elsner, C.; Buchmeiser, M. R. Surfacefunctionalization of plasma-treated polystyrene by hyperbranched polymers and use in biological applications. *J. Appl. Polym. Sci.* **2009**, *112*, 2701−2709.
(35) O'Sullivan, D.; O'Neill, L.; Bourke, P. Direct Plasma Deposition of Collagen on 96-Well Polystyrene Plates for Cell Culture. *ACS Omega* **2020**, *5*, 25069−25076.
(36) Ham, H. O.; Liu, Z.; Lau, K. H. A.; Lee, H.; Messersmith, P. B. Facile DNA Immobilization on Surfaces through a Catecholamine Polymer. *Angew. Chem., Int. Ed.* **2011**, *50*, 732−736.
(37) Valimaa, L.; Pettersson, K.; Vehniainen, M.; Karp, M.; Lovgren, T. A High-Capacity Streptavidin-Coated Microtitration Plate. *Bioconjugate Chem.* **2003**, *14*, 103−111.
(38) Gan, B. K.; Bilek, M. M. M.; Kondyurin, A.; Mizuno, K.; McKenzie, D. R. Etching and structural changes in nitrogen plasma immersion ion implanted polystyrene films. *Nucl. Instrum. Methods Phys. Res., Sect. B* **2006**, *247*, 254−260.
(39) Sharifahmadian, O.; Zhai, C.; Hung, J.; Shineh, G.; Stewart, C. A. C.; Fadzil, A. A.; Ionescu, M.; Gan, Y.; Wise, S. G.; Akhavan, B. Mechanically robust nitrogen-rich plasma polymers: Biofunctional interfaces for surface engineering of biomedical implants. *Mater. Today Adv.* **2021**, *12*, No. 100188.
(40) Kosobrodova, E.; Kondyurin, A.; McKenzie, D. R.; Bilek, M. M. M. Kinetics of post-treatment structural transformations of nitrogen plasma ion immersion implanted polystyrene. *Nucl. Instrum. Methods Phys. Res., Sect. B* **2013**, *304*, 57−66.
(41) Kondyurin, A. V.; Bilek, M. *Ion beam treatment of polymers: application aspects from medicine to space*; 2nd ed.; Elsevier: Amsterdam, Netherlands, 2015.
(42) Kosobrodova, E.; Kondyurin, A. V.; Fisher, K.; Moeller, W.; McKenzie, D. R.; Bilek, M. M. M. Free radical kinetics in a plasma immersion ion implanted polystyrene: Theory and experiment. *Nucl. Instrum. Methods Phys. Res., Sect. B* **2012**, *280*, 26−35.
(43) Yin, Y.; Bilek, M. M. M.; McKenzie, D. R.; Nosworthy, N. J.; Kondyurin, A.; Youssef, H.; Byrom, M. J.; Yang, W. Acetylene plasma polymerized surfaces for covalent immobilization of dense bioactive protein monolayers. *Surf. Coat. Technol.* **2009**, *203*, 1310−1316.
(44) Santos, M.; Filipe, E. C.; Michael, P. L.; Hung, J.; Wise, S. G.; Bilek, M. M. M. Mechanically Robust Plasma-Activated Interfaces Optimized for Vascular Stent Applications. *ACS Appl. Mater. Interfaces* **2016**, *8*, 9635−9650.
(45) Akhavan, B.; Croes, M.; Wise, S. G.; Zhai, C.; Hung, J.; Stewart, C.; Ionescu, M.; Weinans, H.; Gan, Y.; Amin Yavari, S.; Bilek, M. M. M. Radical-functionalized plasma polymers: Stable biomimetic interfaces for bone implant applications. *Appl. Mater. Today* **2019**, *16*, 456−473.

https://doi.org/10.1021/acs.langmuir.2c02573
Langmuir 2023, 39, 343−356

(46) Kondyurin, A.; Naseri, P.; Fisher, K.; McKenzie, D. R.; Bilek, M. M. M. Mechanisms for surface energy changes observed in plasma immersion ion implanted polyethylene: The roles of free radicals and oxygen-containing groups. *Polym. Degrad. Stab.* **2009**, *94*, 638−646.
(47) Yeo, G. C.; Kondyurin, A.; Kosobrodova, E.; Weiss, A. S.; Bilek, M. M. M. A sterilizable, biocompatible, tropoelastin surface coating immobilized by energetic ion activation. *Journal of The Royal Society Interface* **2017**, *14*, 20160837.
(48) Shadpour, H.; Musyimi, H.; Chen, J.; Soper, S. A. Physiochemical properties of various polymer substrates and their effects on microchip electrophoresis performance. *J. Chromatogr. A* **2006**, *1111*, 238−251.
(49) Auld, D. S.; Coassin, P. A.; Coussens, N. P.; Hensley, P.; Klumpp-Thomas, C.; Michael, S.; Sittampalam, G. S.; Trask, O. J.; Wagner, B. K.; Weidner, J. R.; Wildey, M. J.; Dahlin, J. L. In Assay Guidance Manual; Markossian, S. et al., Eds.; *Eli Lilly & Company and the National Center for Advancing Translational Sciences*; National Institutes of Health: Bethesda (MD): 2004.
(50) Tran, C. T. H.; Kondyurin, A.; Chrzanowski, W.; Bilek, M. M. M.; McKenzie, D. R. Influence of pH on yeast immobilization on polystyrene surfaces modified by energetic ion bombardment. *Colloids Surf., B* **2013**, *104*, 145−152.
(51) Kushalkar, M. P.; Liu, B.; Liu, J. Promoting DNA Adsorption by Acids and Polyvalent Cations: Beyond Charge Screening. *Langmuir* **2020**, *36*, 11183−11195.
(52) Saenger, W. *Principles of Nucleic Acid Structure*; Springer Science & Business Media, 2013.
(53) Cholko, T.; Kaushik, S.; Chang, C.-e. A. Dynamics and molecular interactions of single-stranded DNA in nucleic acid biosensors with varied surface properties. *Phys. Chem. Chem. Phys.* **2019**, *21*, 16367−16380.
(54) van Oss, C. J.; Giese, R. F.; Bronson, P. M.; Docoslis, A.; Edwards, P.; Ruyechan, W. T. Macroscopic-scale surface properties of streptavidin and their influence on aspecific interactions between streptavidin and dissolved biopolymers. *Colloids Surf., B* **2003**, *30*, 25−36.
(55) Phillips, M. F.; Lockett, M. R.; Rodesch, M. J.; Shortreed, M. R.; Cerrina, F.; Smith, L. M. In situ oligonucleotide synthesis on carbon materials: stable substrates for microarray fabrication. *Nucleic Acids Res.* **2007**, *36*, e7−e7.
(56) Jin, L.; Horgan, A.; Levicky, R. Preparation of End-Tethered DNA Monolayers on Siliceous Surfaces Using Heterobifunctional Cross-Linkers. *Langmuir* **2003**, *19*, 6968−6975.

https://doi.org/10.1021/acs.langmuir.2c02573
Langmuir 2023, 39, 343−356